Earth's Future

RESEARCH ARTICLE
10.1029/2021EF002603

Special Section:
The Future of Critical Zone Science: Towards Shared Goals, Tools, Approaches and Philosophy

Climate Controls on River Chemistry

Li Li[1], Bryn Stewart[1], Wei Zhi[1], Kayalvizhi Sadayappan[1], Shreya Ramesh[1], Devon Kerins[1], Gary Sterle[2], Adrian Harpold[2], and Julia Perdrial[3]

[1]Department of Civil & Environmental Engineering, The Pennsylvania State University, University Park, PA, USA, [2]Department of Natural Resources & Environmental Science, University of Nevada, Reno, NV, USA, [3]Department of Geology, University of Vermont, Burlington, VT, USA

Key Points:

- Continental-scale river chemistry data show that mean discharge predominantly regulates mean concentrations of 16 solutes
- A simple watershed hydro-biogeochemical reactor model illuminates that river chemistry is driven by the relative rates of solute addition (by reactions and input) and solute export
- Where river discharge dwindles in a warmer climate, higher concentrations will deteriorate water quality even without human perturbations

Supporting Information:

Supporting Information may be found in the online version of this article.

Correspondence to:

L. Li,
lili@engr.psu.edu

Citation:

Li, L., Stewart, B., Zhi, W., Sadayappan, K., Ramesh, S., Kerins, D., et al. (2022). Climate controls on river chemistry. *Earth's Future*, *10*, e2021EF002603. https://doi.org/10.1029/2021EF002603

Received 12 DEC 2021
Accepted 6 MAY 2022

Author Contributions:

Conceptualization: Li Li
Data curation: Gary Sterle, Adrian Harpold
Formal analysis: Li Li, Bryn Stewart, Wei Zhi, Kayalvizhi Sadayappan, Shreya Ramesh

Abstract How does climate control river chemistry? Existing literature has examined extensively the response of river chemistry to short-term weather conditions from event to seasonal scales. Patterns and drivers of long-term, baseline river chemistry have remained poorly understood. Here we compile and analyze chemistry data from 506 minimally impacted rivers (412,801 data points) in the contiguous United States (CAMELS-Chem) to identify patterns and drivers of river chemistry. Despite distinct sources and diverse reaction characteristics, a universal pattern emerges for 16 major solutes at the continental scale. Their long-term mean concentrations (C_m) decrease with mean discharge (Q_m), with elevated concentrations in arid climates and lower concentrations in humid climates, indicating overwhelming regulation by climate compared to local Critical Zone characteristics such as lithology and topography. To understand the C_mQ_m pattern, a parsimonious watershed reactor model was solved by bringing together hydrology (storage–discharge relationship) and biogeochemical reaction theories from traditionally separate disciplines. The derivation of long-term, steady state solutions lead to a power law form of C_mQ_m relationships. The model illuminates two competing processes that determine mean solute concentrations: solute production by subsurface biogeochemical and chemical weathering reactions, and solute export (or removal) by mean discharge, the water flushing capacity dictated by climate and vegetation. In other words, watersheds function primarily as reactors that produce and accumulate solutes in arid climates, and as transporters that export solutes in humid climates. With space-for-time substitution, these results indicate that in places where river discharge dwindles in a warming climate, solute concentrations will elevate even without human perturbation, threatening water quality and aquatic ecosystems. Water quality deterioration therefore should be considered in the global calculation of future climate risks.

1. Introduction

Rivers host a myriad of invisible chemical solutes that define the baseline quality of life-sustaining flowing waters. River chemistry reflects the response of Earth's Critical Zone, the zone from the tree top to the bottom of groundwater, to external climate forcing and human perturbations (Brantley et al., 2017). River water originates from precipitation, most of which infiltrates and flows via subsurface and river corridors (Figure 1). Along its journey, water mobilizes solutes by interacting with roots, microbes, soils, sediments, and rocks. As it eventually exits at river outlets, it carries the chemical signature of its interactions along its flow paths, and reflect the relative magnitude of biogeochemical reactions that produce solutes and export processes that transport solutes (Li et al., 2021).

River chemistry is essential in regulating carbon-climate feedbacks, water quality, and aquatic ecosystem health. Solutes such as dissolved organic and inorganic carbon (DOC and DIC) and nutrients readily transform in rivers and emit greenhouse gases including CO_2, N_2O, and CH_4 (Castellano et al., 2010; Duvert et al., 2018; Hutchins et al., 2020; Raymond et al., 2013; Yao et al., 2020). DOC can also mobilize toxic metals and facilitates the formation of carcinogenic disinfectant by-products during water treatment (Laudon et al., 2012). Nitrogen-containing solutes such as nitrate have persisted for decades, causing algae blooms and dead zones in receiving waters (Brookfield et al., 2021; Van Meter et al., 2018). High cation concentrations from rock weathering can clog pipes via solid precipitates. Water quality degradation can elevate water treatment costs and energy use to beyond the current water-related primary energy consumption of 12.6% in the US (Sanders & Webber, 2012). Deterioration of water quality therefore can present long-term, multi-faceted, and far-reaching threats to aquatic ecosystems, food sources (e.g., fishes), and human society.

Funding acquisition: Li Li, Adrian Harpold, Julia Perdrial
Methodology: Li Li
Visualization: Bryn Stewart
Writing – original draft: Li Li
Writing – review & editing: Li Li, Bryn Stewart, Wei Zhi, Shreya Ramesh, Devon Kerins, Adrian Harpold, Julia Perdrial

Despite its importance, the risks of changing river chemistry and degrading water quality under a warming climate have received marginal attention. An example is the 12-chapter, 1,300-page Intergovernmental Panel on Climate Change Assessment Report 6 (IPCC, 2021). The report discusses changing water chemistry in oceans, including ocean acidification and deoxygenation. The risks of changing chemistry of inland waters that sustain all aquatic and terrestrial lives, including human, have barely been discussed. This is in stark contrast to multiple chapters in IPCC report and extensive literature on the impacts of changing climate on water cycles, climate disasters, and hydrological extremes (AghaKouchak et al., 2021; Bales et al., 2006; Higuera & Abatzoglou, 2021; IPCC, 2021; Paschalis et al., 2020).

Such insubstantial attention on water quality risks may arise from limited understanding on how river chemistry evolves under a changing climate. The common perception is that river chemistry is regulated more by local material abundance instead of climate. For example, concentrations of geogenic solutes (e.g., elements released from rock weathering) are conceived as depending on lithology (Bluth & Kump, 1994; Gaillardet et al., 1999; Ibarra et al., 2016). In contrast, concentrations of biogenic solutes involved in biological processes (e.g., nutrients and carbon), are thought to hinge on vegetation, land cover, and anthropogenic input (Kim et al., 2020; Van Meter et al., 2018; Worrall & Burt, 2007).

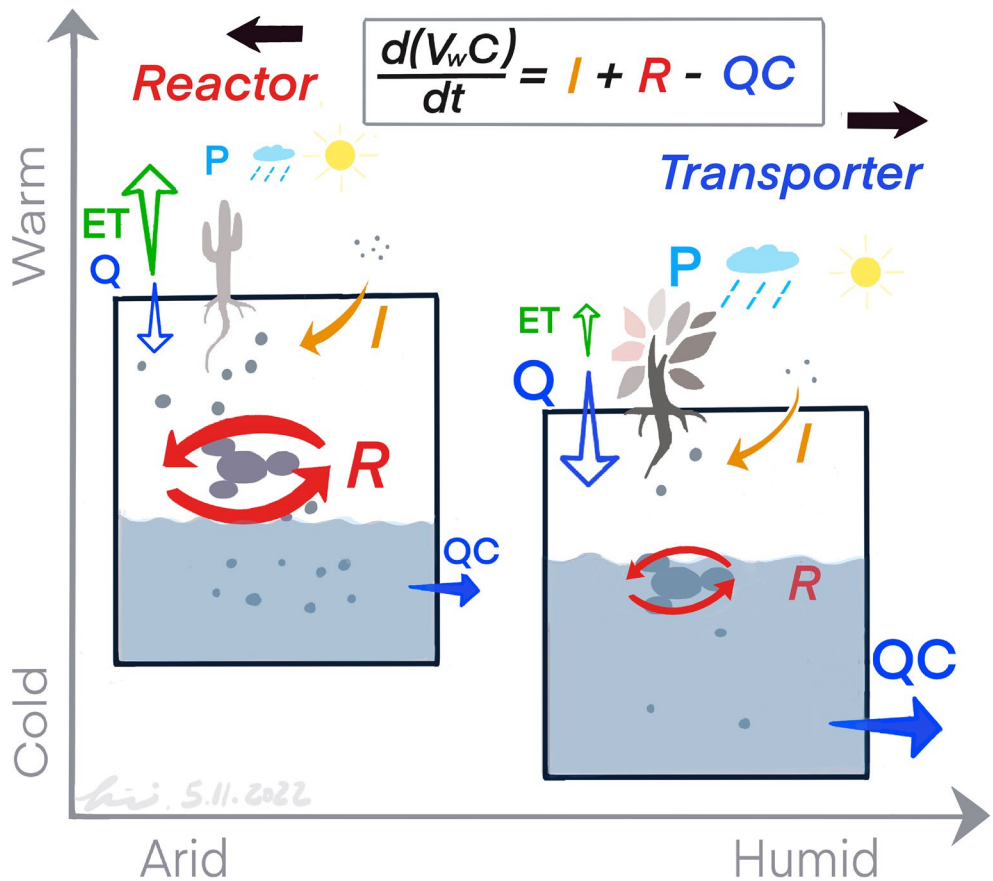

Figure 1. A conceptual model of watershed hydro-biogeochemical reactor under different climates. Water originates from precipitation and travels via subsurface flow paths and river corridors before exiting at river outlets. Along its flow paths, water mobilizes solutes by interacting with roots, microbe, soil, and rocks. The dynamics of solute concentrations in the stored water (V_w) are therefore regulated primarily by two competing processes: the addition of solutes by external input (I) and production of solutes by reactions (R) in soils, rocks, and streams, and the export of solutes by discharge (QC) (Equation 2). External input can happen but are often insignificant in natural, minimally-impacted watersheds. Under warming climate, some places will become more arid, leading to lower river discharge ($Q = P - ET$) and solute export (QC); some places will become more humid, resulting in lower solute concentrations but higher solute export fluxes to rivers. Watersheds function primarily as solute-producing **reactors** in arid, warm climates, and as solute-exporting **transporters** in humid, cold climates.

Existing literature has extensively documented the response of river chemistry to weather conditions in streams and rivers at event to seasonal time scales, often encapsulated in concentration–discharge relationships (Dupas et al., 2016; Ebeling et al., 2021; Godsey et al., 2019; Godsey et al., 2009; Hooper et al., 1990; Knapp et al., 2020; Moatar et al., 2017; Pinder & Jones, 1969). Geogenic solutes often exhibit dilution patterns where concentrations decrease with discharge or chemostatic patterns where concentrations vary negligibly compared to discharge (Godsey et al., 2009; Ibarra et al., 2016; Torres & Baronas, 2021). On the other hand, biogenic solutes such as DOC often exhibit flushing patterns where concentrations increase with discharge (Boyer et al., 1997; Herndon et al., 2015; Zarnetske et al., 2018). The response of nitrate concentrations to discharge varies with land uses: flushing patterns emerge in most agriculture sites, whereas diverse patterns have been observed in natural rivers with minimal human influence (Botter et al., 2020; Ebeling et al., 2021; Moatar et al., 2020; Zhi & Li, 2020). Mounting evidence has shown that these contrasting patterns arise from the influence of changing weather, flow paths, and distinct source water chemistry in shallow soils and in deeper groundwater (Seibert et al., 2009; Zhi et al., 2019; Zimmer & McGlynn, 2018).

Long-term river chemistry response to different climate conditions however has been scarcely studied. Riverine mean concentrations of geogenic solutes have been observed to decrease from arid to humid climates (Maher & Chamberlain, 2014; White & Blum, 1995).These concentration variations have been explained by the thermodynamic limits of chemical weathering and the approach to equilibrium at long water travel times under arid climates (Ibarra et al., 2016; Maher & Chamberlain, 2014). More recently, a wide range of solutes has been shown to similarly exhibit dilution patterns across climate gradients, with high concentrations under arid climates (Godsey et al., 2019). This has been postulated to depend on the time scales of soil buffering. In general, however, we lack conceptual framework and quantitative approaches that can mechanistically explain and project baseline concentrations for solutes of diverse origins.

How does climate control river chemistry? With space-for-time substitution, answers to this question can help project river chemistry in the future climate. Our aim is to identify patterns across climate gradients and understand predominant control of river chemistry at the continental scale. We compile and analyze chemistry data from 506 minimally-impacted rivers (412,801 data points) in the contiguous United States. In doing so we focus on the effects of climate without the entangled effects of human perturbation. We calculate long-term, baseline concentrations of pervasive solutes of diverse origins for each river. We further derive solutions to a parsimonious watershed hydro-biogeochemical reactor model to explain the observed patterns and quantitatively depict the relationship between long-term mean concentrations and mean specific discharge, a key measure of climate conditions.

2. Methods

2.1. The CAMELS-Chem Database

This work compiled a new dataset CAMELS-Chem. The new dataset augments the existing CAMELS (Catchment Attributes and Meteorology for Large-sample Studies) dataset (Addor et al., 2017), and comprises the U.S. Geological Survey chemistry data (412,801 data points, 1980 to 2014) from 506 minimally-impacted rivers (Sterle et al., 2022). It pairs atmospheric deposition and water chemistry data with the existing CAMELS (Catchment Attributes and Meteorology for Large-sample Studies) dataset, therefore filling the need of a data set with complementary watershed attributes, river water flow, and river chemistry data. The dataset includes 18 common river chemistry constituents: Al, Ca, Cl, DOC, Total Organic Carbon (TOC), HCO_3, K, Mg, Na, Total Dissolved Nitrogen [nitrate + nitrite + ammonia + organic-N], total organic nitrogen (TON), nitrate (NO_3), dissolved oxygen (DO), pH (field), pH_l (lab), Si, SO_4, and water temperature. This work used data of all solutes except DO, a solute that depends largely on river temperature, light, and flow dynamics (Bernhardt et al., 2018; Zhi et al., 2021), and pH_l (lab) that is similar to pH (field).

The solutes are loosely categorized based on their origins into biogenic (from soil biogeochemical reactions) and geogenic groups (from chemical weathering). The solute HCO_3 can be biogenic from soil respiration (that produces soil CO_2) and geogenic from carbonate weathering. Its concentration limits however are controlled by the thermodynamics of carbonate minerals and is therefore grouped into geogenic solutes.

The mean concentrations (C_m) of each solute were calculated as the arithmetic mean of available concentration data at each site in CAMELS-Chem. We purposely choose to use arithmetic mean, instead of the commonly used

flux-normalized mean concentrations (Godsey et al., 2019; Ibarra et al., 2016; White & Blum, 1995), because arithmetic mean gives equal weight to every data point. Flux-normalized mean concentrations are weighted by fluxes (discharge) that often vary by orders of magnitude, and therefore give more weight to concentrations at high discharge. This could lead to more biased mean concentrations, especially when the timing and frequency of sampling are inconsistent across different discharge regimes at different sites.

2.2. The Long-Term Energy and Water Balance of Watersheds

The amount of precipitated water (in both rainfall and snowfall forms) that eventually ends up in streams and rivers, or mean discharge, is influential in regulating water travel time and the extent of interactions among water, soil, and rocks, and therefore river chemistry (Ibarra et al., 2019; Keller, 2019; Li et al., 2021). Here we relate mean solute concentrations to climate conditions at each site using a widely used relationship, Budyko equation. Various forms of Budyko equations relate the long-term ratio of evaporative index to aridity index (Chen & Sivapalan, 2020; Gentine et al., 2012; Reaver et al., 2020). Here we used the original form (Budyko, 1974):

$$\frac{ET}{P} = \frac{1}{\left[\left(\frac{P}{PET}\right)^{\beta} + 1\right]^{1/\beta}} \tag{1}$$

where P is precipitation, ET is evapotranspiration, the summation of evaporation (from open water, bare soil, and vegetated surfaces), transpiration (from within plant leaves), and sublimation from ice and snow surfaces. Evapotranspiration is regulated by the land-surface interactions that determine the exchange of energy and water between land surface and atmosphere. The climatic potential ET (PET) measures the "drying power" regulated by both climate and land cover (Dingman, 2015). The dimensionless parameter β modifies the curvature of the evaporative index ET/P as a function of aridity index PET/P.

The CAMELS-Chem dataset includes PET, mean annual precipitation (P), and mean annual specific discharge ($Q_{m,}$ thereafter mean discharge) for each site. Actual evapotranspiration (ET) was calculated as the difference between P and Q_m, assuming water-balanced watersheds.

2.3. The Watershed Hydro-Biogeochemical Reactor Model

Broadly, we can consider mean river chemistry as reflecting the response of long-term, baseline chemistry to climate, and their instantaneous variations from event to seasonal scales as reflecting its response to rapidly changing weather conditions. We can conceptualize watersheds as well-mixed hydro-biogeochemical reactors (Figure 1). Solutes can come from external input such as atmospheric deposition and/or human input such as the addition of nutrients from agriculture or urban watersheds. As meteoric water infiltrates and travels through subsurface and river corridors, it mobilizes solutes by interacting with materials along its flow paths (at rates R), and ultimately exports solutes at the rates QC.

The governing equation and solutions. The mass conservation of an arbitrary solute in a well-mixed watershed reactor can be written as follows:

$$\frac{d(V_w C)}{dt} = I + R - QC \tag{2}$$

Here V_w is water volume per drainage area (m^3 water/m^2 drainage area); C is aqueous concentration of the solute (g/m^3 water, equivalent to mg/L water); I is external input rate (g/m^2 drainage area/yr) (orange arrows across the land surface, Figure 1), which can be dry or wet deposition or both in a minimally-impacted watershed; R is net rate of reactions (g/m^2 drainage area/yr, red arrows) that produce or consume the solute; and Q is specific discharge (m^3 water/m^2 drainage area/yr, dark blue arrows in Figure 1). Individual solutes are often involved in multiple reactions. In the simple representation of Equation 2, the single R term may lump multiple reactions and can be considered as the net reaction rate of multiple reactions. For a water-balanced watershed, $Q = P - ET$, where P and ET are precipitation and evapotranspiration (m^3 water/m^2 drainage area/yr, light blue and green arrows in Figure 1), respectively.

As detailed in Supporting Information S1, the time-dependent analytical solution to Equation 2 is

$$C(t) = C_m + [C_0 - C_m]\, e^{-\frac{t}{\tau_w}}, \text{where } C_m = \frac{I_m + R_m}{Q_m} \quad (3)$$

Here C_m is the long-term, steady state, baseline mean concentration in individual sites. The second term $[C_0 - C_m]e^{-t/\tau_w}$ is time dependent with an exponential form. The characteristic time $\tau_w = V_w/Q_m$ quantifies the mean water travel time from its entry on land to its exit point (river) in a watershed (Rinaldo et al., 2015; Sprenger et al., 2019; Tetzlaff et al., 2009). If time is sufficiently long (large t), the exponential term approaches zero such that the concentration becomes $C_m = (I_m + R_m) / Q_m$, the steady state solution. For example, when $t = \tau_w$, $e^{-t/\tau_w} = 0.37$; when $t = 3\tau_w$, $e^{-t/\tau_w} = 0.05$. That is, when the time is longer than a few times of τ_w, the second term becomes negligible.

Almost all solutes have varied sources. Solutes such as Cl, SO_4, and NO_3 may have comparably larger atmospheric input (I) than other solutes. In urban and agricultural sites, the human input of nutrient-containing solutes can be significant. In minimally-impacted watersheds here, the external input however tends to be low compared to productions from reactions in the subsurface (Berner & Berner, 2012). We therefore focus primarily on the reaction rate R as the major source. In that case, the mean concentration has the following form with mean reaction rate R_m and mean discharge Q_m:

$$C_m = \frac{R_m}{Q_m} \quad (4)$$

Equation 4 reveals that long-term, steady-state mean concentrations are regulated by the relative magnitude of two processes. One is the reactions in the subsurface or in river corridors that produce a solute (at rate R_m), the other is the export process that carries a solute out of the watershed at the river exit (at rate Q_m). High R_m and low Q_m result in high concentrations, and low R_m and high Q_m lead to low concentrations in subsurface and by extension in rivers. This equation can be used broadly as an organizing framework to understand competing processes that regulate baseline solute concentrations.

The C_mQ_m relationships: the response of river chemistry to climate. The values of R_m at the watershed scale are typically unknown. We do know the functional dependence of rates on measurable variables such as temperature, soil moisture, material abundance, intrinsic rates, and aqueous geochemistry from reaction kinetic theory. We can combine theories from hydrology and reaction kinetics and thermodynamics from biogeochemistry for different groups of solutes based on their origin and reaction types (details below and in Supporting Information S1) to derive steady state relationships between C_m and Q_m in the form of Equations 5 and 6.

For biogenic solutes, the derivation of C_mQ_m relationship involved the use of water storage-discharge relationships from hydrology and reaction kinetics with dependence on temperature and water content (or soil moisture) from biogeochemistry. The reaction rate R_m depends on temperature (T) and soil moisture (or water content S_w) (Davidson et al., 1998; Mahecha et al., 2010). The rate dependence on water content takes the general form $R_m = R_0 = k_0 S_A f(T) f(S_w)$, where k_0 is the maximum reaction rate constant, S_A is the surface area that quantifies the abundance of organic materials, $f(T)$ describes the rate dependence on temperature, which can take the form of Q_{10} formula (e.g., $f(T) = Q_{10}{}^{(T-20)/10}$, Lloyd & Taylor, 1994), and $f(S_w)$ describes the rate dependence on soil moisture. Reactions such as soil respiration and carbon decomposition often reach maxima at intermediate water content (e.g., soil moisture of 0.5–0.7 in many places) (Yan et al., 2018), because rates tend to be low under extremely dry and wet conditions. The mean soil moisture in particular locations and at the watershed scale however rarely become higher than 0.5, even in wet places and at wet times (e.g., Lin et al., 2006). We therefore use a simple form $f(S_w) = (S_w)^n$, where the exponent n quantifies the sensitivity of reaction rates to water content. Water content (or storage) and discharge can be linked by storage-discharge relationships in various forms (Kirchner, 2009). Here we use a simple form $Q = \alpha_0 S_w^{\beta_0}$ (Wittenberg, 1999). Large β_0 values indicate rapidly changing discharge responding to changes in S_w, whereas small β_0 values indicate relatively stable discharge that varies insignificantly with S_w.

With these reaction rate laws and functional dependence, the following C_mQ_m relationship can be derived for biogenic solutes (details in Supporting Information S1):

$$C_m = AQ_m{}^B, \text{ where } A = k_0 S_A f(T) \alpha_0{}^{\left(-\frac{n}{\beta_0}\right)}, \quad B = \frac{n}{\beta_0} - 1 \tag{5}$$

The parameter A is a bulk measure of reaction rates and combines several rate-related parameters, including reaction rate constant k_0, surface area S_A, rate dependence on soil moisture n and temperature $f(T)$, and parameters in S_w-Q relationships. The parameter B is determined by the ratio of the rate dependence on water content (n) and discharge dependence on water content (β_0). The B value quantifies concentration sensitivity to variations in mean discharge. Here the symbols A and B are used to differentiate from the a and b in the instaneous CQ relationships $C = aQ^b$.

For geogenic solutes, weathering reaction kinetics follow the transition state theory with a thermodynamic limit term $R_m = R_0(1 - C/C_{eq})$, with the last term indicating the distance from reaction equilibrium (Lasaga, 1998; Lasaga et al., 1994). This rate law leads to the following equation (details in Supporting Information S1):

$$C_m = \frac{C_{eq} Da}{1 + Da} = \frac{C_{eq} R_0}{Q_m C_{eq} + R_0} \tag{6}$$

where $Da = \tau_w/\tau_{eq}$, the dimensionless Damköhler number that quantifies the relative magnitude of water travel time (τ_w) and the time to reach equilibrium $\tau_{eq} = C_{eq} V_w/R_0$. This equation builds upon a rich history of reactive transport formulation in literature for geogenic solutes with thermodynamic limits (Ibarra et al., 2016; Maher, 2011; Maher & Chamberlain, 2014; Salehikhoo et al., 2013; Steefel, 2007; Torres & Baronas, 2021; Wen & Li, 2017; Wen & Li, 2018; Wymore et al., 2017).

Under the conditions that τ_w is small (humid climate) or τ_{eq} is large (e.g., for silicate weathering), $Da << 1$, reaction is far from equilibrium, Equation 6 becomes $C_m = C_{eq} Da = C_{eq} \times ((V_w/Q_m)/(V_w C_{eq}/R_0)) = R_0/Q_m = R_m/Q_m$. This equation has the same form as Equation 4 for biogenic solutes and can be further rearranged into the same form of Equation 5 with parameters specific for weathering reactions. For example, weathering of rocks such as silicates, shale, and evaporites releases cations (Na, K, Si, and Al) and anions (Cl, SO_4, HCO_3). These reactions lead to the precipitation of clay, effectively reducing concentrations of solutes from silicates such that they hardly reach reaction equilibrium.

For geogenic solutes involved in carbonate weathering (Ca, Mg, and HCO_3, and pH), they can rapidly reach equilibrium such that their $C_m Q_m$ relationships follow Equation 6. For these solutes, when τ_w is small (humid climate), $Da << 1$, C_m decreases with increasing Q_m and depends on R_0. Arid climates entails that $\tau_w >> \tau_{eq}$ and $Da >> 1$, such that Equation 6 becomes $C_m = C_{eq}$.

2.4. Model Assumption, Implications, and Utilities

The model conceptualizes watersheds as well-mixed reactors that drain to rivers. It is meant to broadly capture controls of long-term, baseline mean concentrations. It is not meant to represent detailed short-term temporal dynamics and spatial structure such as flow paths and source water chemistry at different subsurface depths. In-stream processes may also influence concentrations, especially under low flow conditions (Dodds, 2006; Perdrial et al., 2014). In-stream reaction processes are implicitly counted for as in the governing Equation 2, as one can consider in-stream reactions as contributing partially to R_m. The parsimonious representation entails a slim number of parameters and salient relationship that reveal first-order mechanisms. As we will illustrate in Section 3, these relationships capture concentration variations across climate gradients and reveal competing mechanisms that ultimately drive river chemistry.

For solutes that are not thermodynamically limited by equilibrium, the derivation here accidently arrives at a power law form ($C_m = AQ_m{}^B$). This $C_m Q_m$ power law relationship however differs from the short-term, instantaneous CQ patterns ($C = aQ^b$) at event to seasonal time scales that have been extensively studied in literature, as we will elaborate more in Section 4. It depicts the dependence of long-term, baseline concentration on mean discharge at annual time scales and beyond.

Although this work focuses on minimally-impacted watersheds, the application of the model is not limited to such watersheds. For example, the input term I in Equation 2 is loosely defined: it can be atmospheric input and/or human input such as the addition of nutrients in agriculture or urban watersheds. The long-term accumulation

of nutrients on agriculture lands can also change some of reaction parameters, for example, the surface area S_A that quantifies the abundance of nitrogen- and phosphorus-containing materials. The model can be used broadly as an organizing framework to understand competing processes that regulate mean solute concentrations. More complex reactive transport models at the watershed scale can be used to complement such simple models and to examine detailed processes, variables, and spatial heterogeneities that reflect idiosyncrasies of specific sites (Li, 2019; Wen et al., 2021; Wen et al., 2020).

3. Results

3.1. Large Concentration Variations at the Continental Scale

The compiled data indicate that mean discharge varies by three orders of magnitude and is higher in the eastern US and along the coasts, and lowest in the Great Plains from North Dakota down to Texas (Figure 2). Mean concentrations also vary by orders of magnitude across sites, depending on specific solutes. They are highest in the Great Plains for many solutes, including Cl, SO_4, and cations (e.g., Na, K, Ca, and Mg). Concentrations are typically higher in arid climates and lower in humid climates, although considerable variations occur. Although eastern US has historically received more acid deposition (Berner & Berner, 2012), rivers in the western US generally have higher SO_4 concentrations, possibly due to gypsum from evaporites and lack of dilution due to low discharge. NO_3 concentrations are highest in mid-west Corn Belt area, possibly elevated by dust and dry deposition from nearby agricultural areas.

3.2. Biogenic Solutes: Higher Concentrations at Lower Mean Discharge

Biogenic solutes include TOC, DOC, TON and dissolved organic nitrogen (DON), total nitrogen (TN), and nitrate (NO_3) (Figure 3). They are primarily involved in vegetation- and microbe-mediated reactions including soil respiration, nitrification, and denitrification. Some solutes, including NO_3, also come from atmospheric deposition and fertilizer application (Berner & Berner, 2012). The climate conditions of these rivers cover a wide range, as manifested in evaporative (ET/P) and aridity index (PET/P) values (red lines in left figures of each pair, Figure 3). Concentrations decrease as mean discharge increases and are typically higher under arid climates with high ET/P and PET/P (Figure 3, right). Red lines in the right figures of Figure 3 depict the C_mQ_m relationship $C_m = AQ_m^B$ (Equation 5) at different A and B values. The prediction lines generally capture the trend and range of concentration variation with mean discharge.

Values of B vary across solutes, indicating distinct sensitivity to mean discharge variations. For TOC and DOC, B values are close to −0.9; for TON and DON, they are around −0.5 to −0.6. Organic carbon is typically more abundant than nitrogen-containing solutes in natural systems. Carbon- and nitrogen-containing solutes also experience distinct reactions with different rate sensitivity to temperature and water content. These differences could lead to dissimilar B values and sensitivity to mean discharge. At similar discharge, concentrations vary considerably and hinge upon mean reaction rates, as indicated by the red lines with different A values. The model inferred that rates of TOC and DOC vary from 0.1 to 5 g/m^2/yr, whereas the rates of nitrogen-containing solutes are typically one to two orders of magnitude lower. This is in fact consistent with the observed range of C:N ratios between 1 and 100 (Cleveland & Liptzin, 2007), as carbon is much more abundant than nitrogen in natural soils.

3.3. Geogenic Solutes Without Limits: Elevated Concentrations at Higher Aridity

Soil and rock weathering release cations (Na, K, Si, and Al) and anions (Cl, SO_4, HCO_3). Solutes such as Cl, NO_3, and SO_4 can also cone from rainfall, dust, and pollution sources (e.g., acid rain), although atmospheric deposition is considered low compared to weathering (Berner & Berner, 2012). Weathering of silicates, shale, and evaporites rarely reach equilibrium such that the C_mQ_m relationships of solutes from these rocks have the same form as those of biogenic solutes ($C_m = AQ_m^B$, Equation 5). The concentrations of these solutes are similarly higher in arid environments (Figure 4 left figure of each pair) and decrease with discharge (Figure 4 right figure of each pair).

The data and model solution indicate that the reaction rates (A values) vary by orders of magnitude, with more abundant solutes having higher rates. For anions, the values of A vary from 0.1 to 10 g/m^2/yr for Cl and 0.2–25 g/m^2/yr for SO_4. Among cations, Na and Al have the highest (0.03–1) and lowest (0.0002–0.1 g/m^2/yr) A values, respectively. This is expected, as Na is highly soluble and has the highest concentration range of all

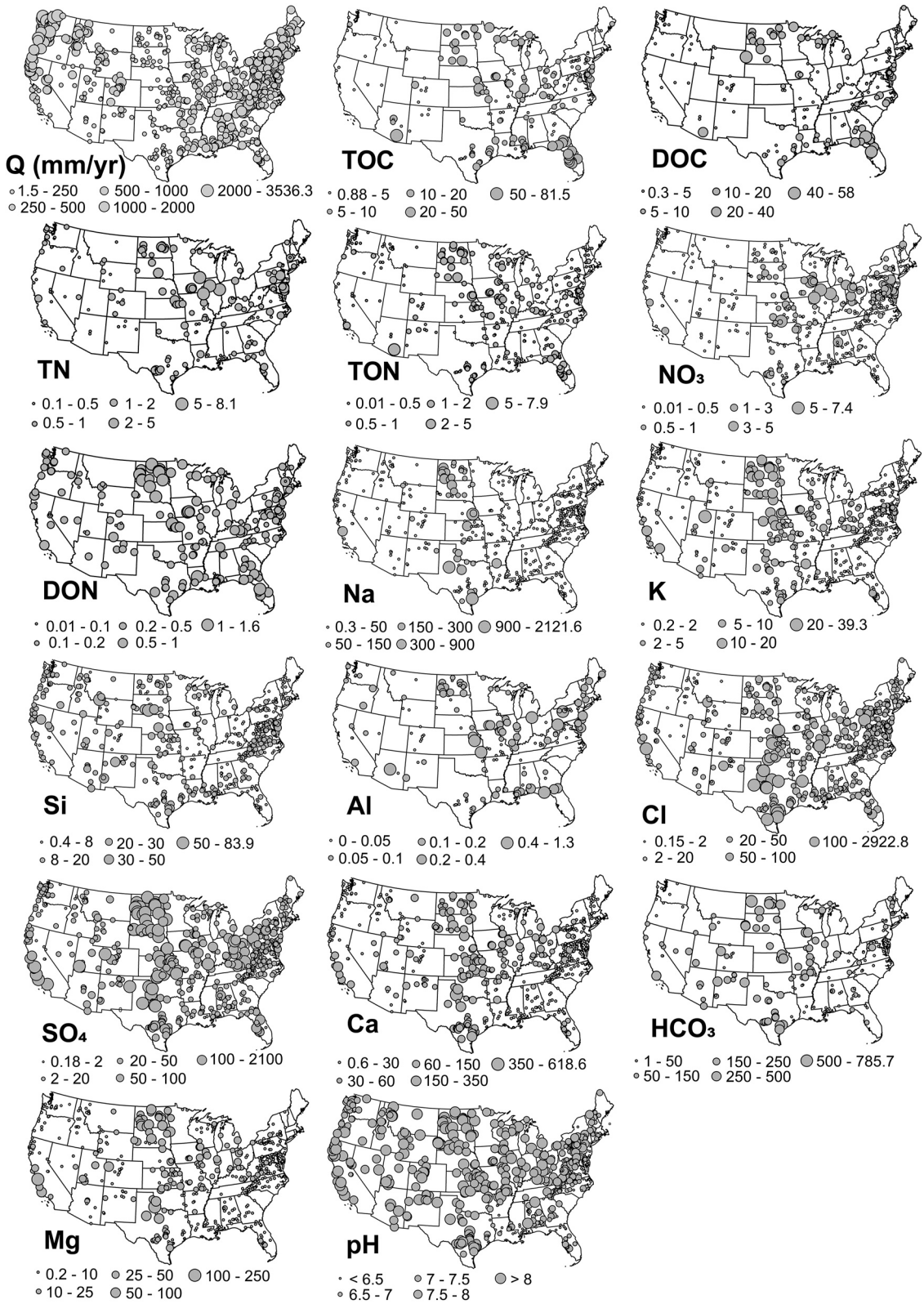

Figure 2. Maps of mean specific discharge (mm/yr) (top left) and mean concentrations (mg/L). Annual mean discharge varies from 1.5 to 2,000 mm/yr, notably lowest in the Great Plains from North Dakota down to Texas. Mean concentrations are higher under arid climates, and are highest in the Great Plains for many solutes.

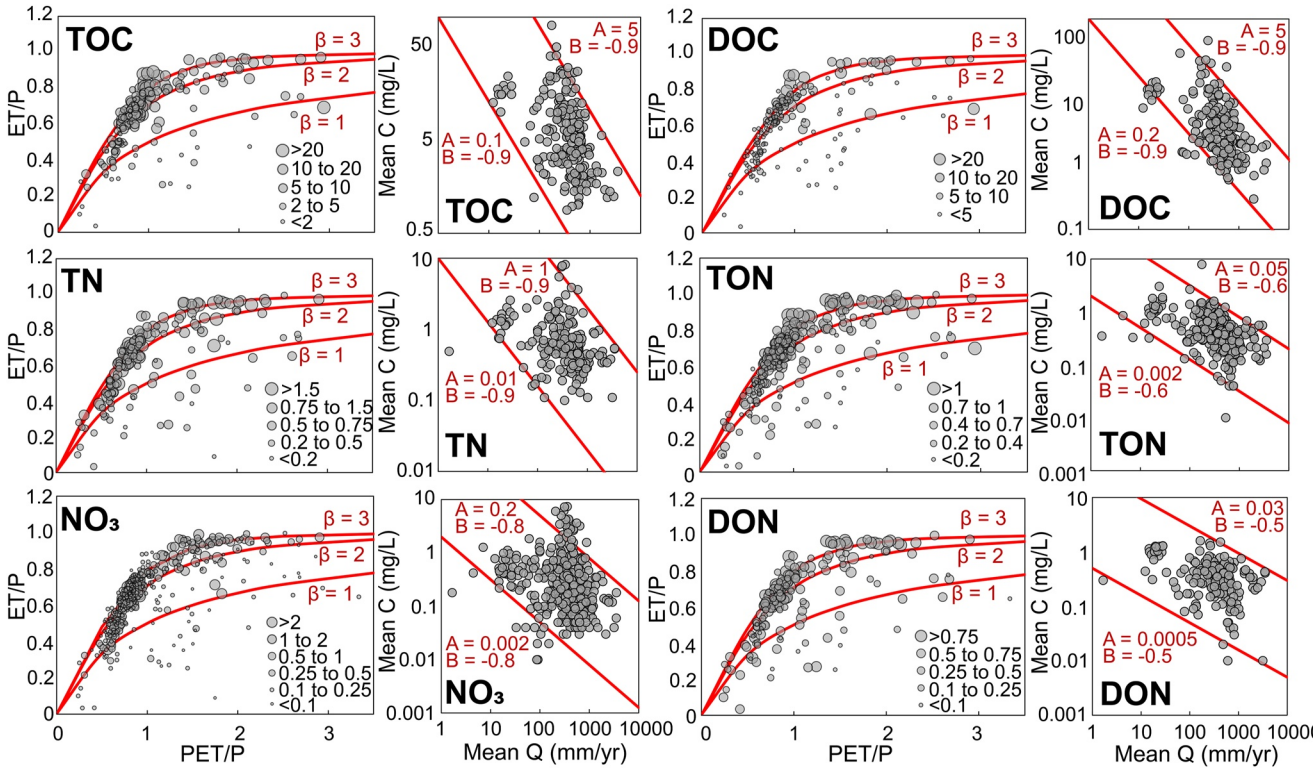

Figure 3. Biogenic solutes. Each solute has one pair of figures. The left figure of each pair is mean concentrations C_m within the Budyko framework. Red lines from Equation 1 with different non-linearity indicator β. The positions of circles are determined by evaporative index (ET/P) and aridity index (PET/P) of each site. Water limitation under arid climates lead to high ET/P and PET/P, meaning most precipitation returns to the atmosphere to meet the climate and vegetation demand for water. The circle sizes indicate concentration levels. The right figure of each pair is the mean concentration (C_m) versus mean discharge (Q_m) data (gray circles). The red lines are from Equation 5, $C_m = AQ_m^B$, where parameter A is a bulk measure of reaction rates (g/m^2/yr), and B reflects the sensitivity of C_m to variations in Q_m. Although with considerable variations, concentrations are typically higher in arid climates and decrease with discharge.

cations. In contrast, Al released from silicate dissolution is usually immobilized rapidly via clay precipitation. Equation 5 also predicts that B values of Na and K are around −0.6 and −0.5, whereas that of Si is around −0.2. The B values of Cl and SO_4 are close to −1. Cl can come from dissolution of evaporites. SO_4 can originate from atmospheric acid deposition but also from pyrite oxidation in shale and gypsum dissolution (Berner & Berner, 2012). These source rocks dissolve rapidly with high solubility. In particular, pyrite dissolution is known to hinge upon the rise and fall of water tables and the availability of oxygen (Crawford et al., 2019). These characteristics can lead to its high sensitivity to discharge and therefore more negative B values.

3.4. Geogenic Solutes From Carbonate Weathering: Higher Concentrations at Higher Aridity but With Limits

Geogenic solutes related to carbonate weathering (Ca, Mg, and HCO_3, and pH) can reach equilibrium rapidly because of high reaction rates. Their C_mQ_m relationship (Equation 6) indicates a form of dependence on mean discharge that differs from biogenic and non-thermodynamic-limiting geogenic solutes discussed in the previous section. Instead of monotonic increase with decreasing discharge, values of C_m reach maxima at a threshold discharge. Data in Figure 5 confirm the existence of such threshold: at Q_m > ~200 mm/yr, concentrations decrease sharply with discharge. Carbonate as a parent rock mostly occurs in Midwestern US (Moosdorf et al., 2010). However, pedogenic carbonate is known to prevail in dry soils in the western US and under arid climates around the globe (Monger et al., 2015; Zamanian et al., 2016). Concentrations of each solute vary considerably, depending on the reaction rate R_0 and equilibrium constant C_{eq}. Pedogenic carbonates often have different solubility due to dust and impurities (Macpherson & Sullivan, 2019), and therefore can have variable C_{eq}

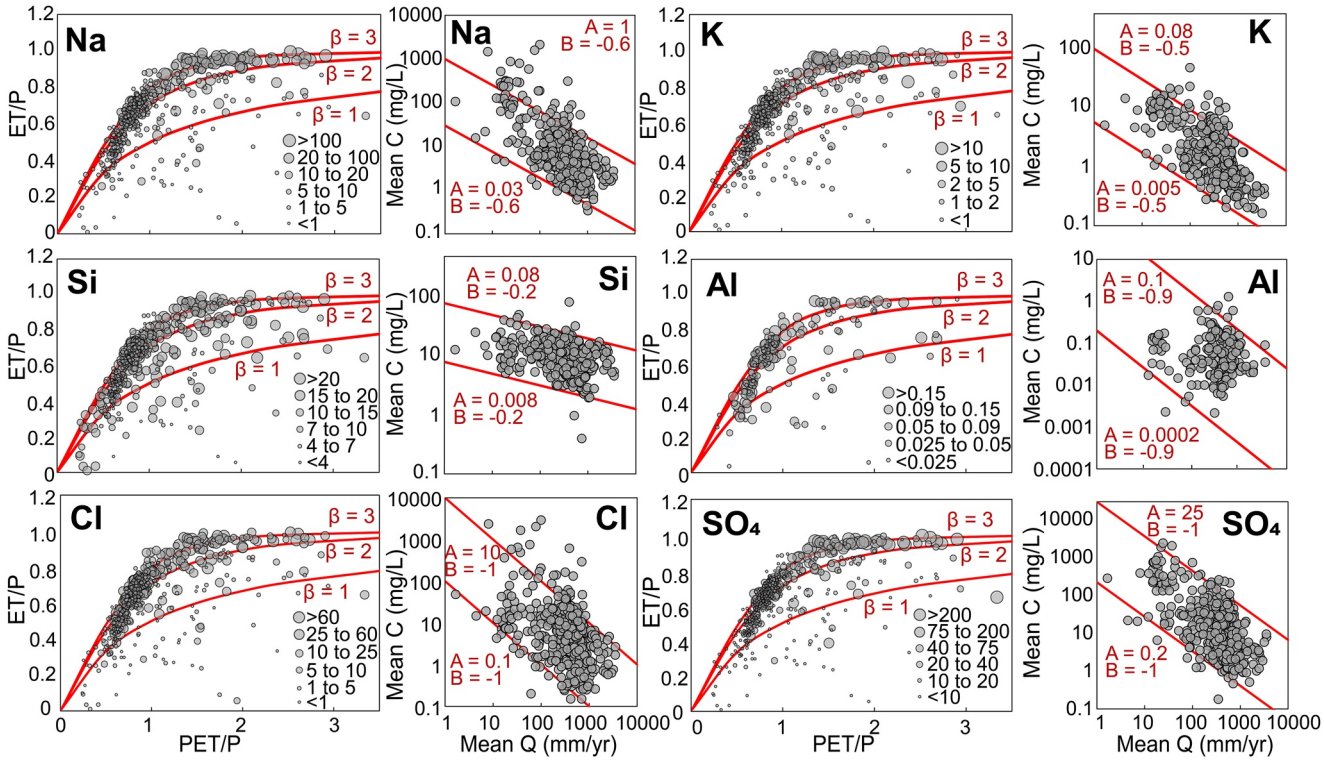

Figure 4. Geogenic solutes without thermodynamic limitation. Each solute has one pair of figures. The left figure of each pair is C_m within the Budyko framework. Red lines are from Equation 1 with different non-linearity indicator β. The positions of circles are determined by evaporative index (ET/P) and aridity index (PET/P). The right figure of each pair is mean concentration C_m versus mean discharge Q_m data (gray circles). The red lines are from Equation 5, $C_m = AQ_m^B$, where parameter A is a bulk measure of reaction rates (g/m^2/yr), and B reflects the sensitivity of C_m to variations in Q_m. Although with considerable variations, concentrations are higher in arid climates and decrease with increasing discharge.

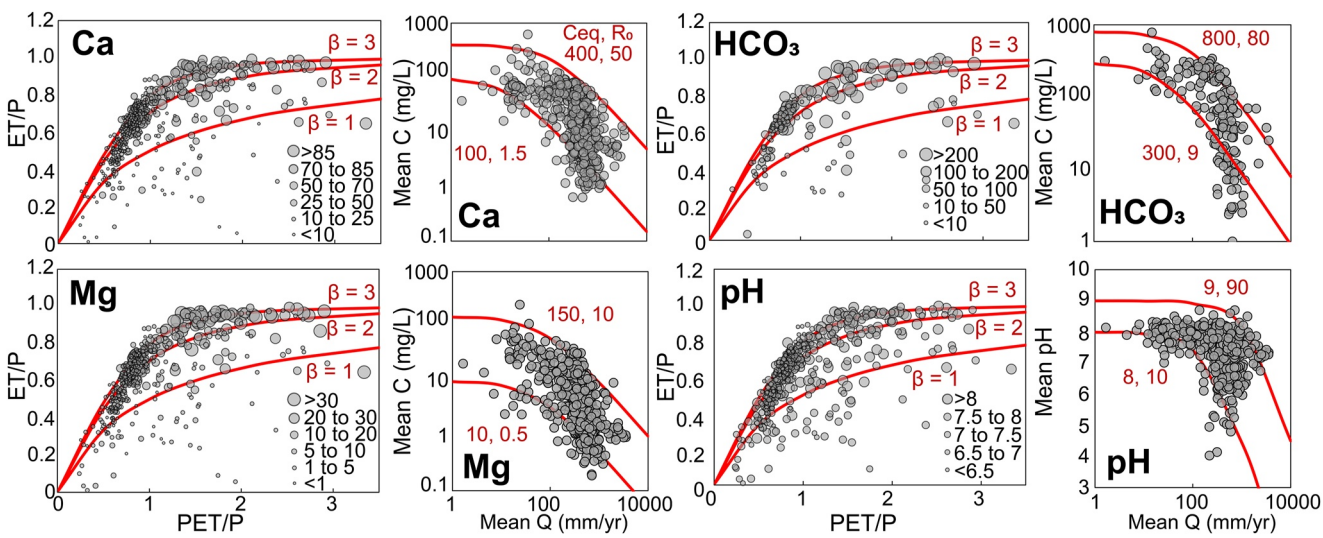

Figure 5. Geogenic solutes from carbonate weathering. Each solute has one pair of figures. The left figure of each pair includes C_m within the Budyko framework. Red lines are from Equation 1. The right figures are C_m versus Q_m data (gray circles). Red lines are from Equation 6, $C_m = C_{eq}R_0/(Q_mC_{eq} + R_0)$, with different equilibrium concentrations C_{eq} (mg/L) and reaction rates R_0 (g/m^2/yr). Mean concentrations increase with decreasing Q_m until reaching maxima at a threshold Q_m around 200 mm/yr.

Table 1
Summary of Parameters in Equations 5 and 6 for All Solutes

Solute	A (g/m^2/yr)	B
TOC	1.1~5	−0.9
DOC	0.2~5	−0.9
TN	0.01~1	−0.9
TON	0.002~0.05	−0.6
NO_3	0.002~0.2	−0.8
DON	0.0005~0.03	−0.5
Na	0.03~1	−0.6
K	0.005~0.08	−0.5
Si	0.008~0.08	−0.2
Al	0.0002~0.1	−0.9
Cl	0.1–10	−1
SO_4	0.2–25	−1
Solute	R_0 (g/m^2/yr)	C_{eq} (mg/L)
Ca	1.5~50	100~400
HCO_3	9~80	300~800
Mg	0.5~10	10~150
pH[a]	10~90	8~9

[a]R_0 values for pH are not particularly meaningful as pH is a negative log. The C_{eq} values of pH however indicate that the upper limits of pH values in US rivers are around 8–9.

values. Between solutes, HCO_3 has the highest R_0 and C_{eq}, possibly because HCO_3 can also come from biological processes such as soil respiration in addition to carbonate weathering.

4. Discussion

4.1. Climate Regulation of River Chemistry: Watersheds as Reactors in Arid Climates and Transporters in Humid Climates

This work used a large data set to identify patterns of baseline river chemistry at the contiguous United States. A universal C_mQ_m pattern emerges: mean concentrations of all 16 solutes increase with aridity and decrease with increasing mean discharge. This pattern contrasts the general perception that river chemistry is primarily controlled by local material abundance in the Critical Zone, including lithology (Gaillardet et al., 1999), vegetation, and organic matter (Raymond et al., 2008; Van Meter et al., 2018; Worrall & Burt, 2007).

A watershed hydro-biogeochemical reactor model was solved analytically to understand the processes that drive the pattern. The derivation of the solution and C_mQ_m relationships (Equations 5 and 6) brings together theories from traditionally separate disciplines: storage-discharge relationship in hydrology and reaction kinetics in biogeochemistry and chemical weathering. The steady state solution illuminates two competing processes that drive the continental-scale pattern (Equation 4, Figure 1): solute addition via reactions (and possibly input), and solute export by discharge. Equation 4 indicates that in arid climates, reaction rates R_m are higher compared to Q_m, leading to high C_m. In other words, watersheds function as reactors that primarily produce and accumulate solutes. In contrast, in humid climates, reaction rates R_m are higher compared to Q_m, leading to low C_m. Watersheds therefore mostly function as transporters that export solutes.

Such solution has been developed before for geogenic solutes (chemical weathering solutes) (e.g. Maher & Chamberlain, 2014) but not for biogenic solutes such as carbon and nutrient solutes. The dilution patterns of geogenic solutes, where high concentrations under arid climates and lower, rapidly decreasing concentrations under humid climates, echo earlier observations in literature (Maher & Chamberlain, 2014; White & Blum, 1995). This work therefore brings a unified framework for solutes of both biogenic and geogenic origins.

The model underscores the first-order control of mean discharge and the secondary influence of material abundance, as expressed in reaction rate parameters (A or R_0). As shown in Table 1, the A values are lowest (0.0002–0.1 g/m^2/yr) for Al, which happens to have the lowest concentration range. The A values are highest (9–80 g/m^2/yr) for HCO_3, which also has the highest concentration range. In other words, high A or R_0 indicate rapid solute production and high concentrations. This is hardly surprising, as these values encapsulate the intertwined influence of reactivity (k_0), mineral abundance (S_A), climate ($f(T)$), and water flow (α_0) (Equations 5 and 6). For biogenic solutes, values of A may also indicate the quantity and quality of organic matter (and therefore vegetation) and microbial communities. The lumped nature of A and R_0 however alludes to the challenges of differentiating the influence of individual factors.

The sensitivity of concentrations to discharge variation is quantified by the value of B ($= n/\beta_0 - 1$), which depends on the reaction rate dependence on water content (n) and discharge dependence on water content (β_0). The former (n) likely hinges upon solute origin and chemical properties of materials (e.g., organic matter and minerals) that produce solutes. In particualr, Cl and SO_4 have B values of 01, potentially indicating they are primarily from external atmospheric input in many sites (see Equation S3 for mostly airborne solutes). The latter (β_0) depends on the physical structure that regulates water storage and flow generation. For example, steep topography and clay-rich soils respond rapidly to precipitation and have high β_0 values (Kirchner, 2009; Wlostowski et al., 2021; Xiao et al., 2019). When $n > \beta_0$, or reaction rates are more sensitive to water content than discharge, $B > 0$;

when $n < \beta_0$, or reaction rate is less sensitive to water content than discharge, $B < 0$. Values of B are negative for all solutes, indicating reaction rates are less sensitive to water content than discharge. This is expected, as discharge predominately depends on water content, whereas reaction rates depend on an array of factors other than water content, which may subdue the impacts of water content. Overall, the expression of B underscores the importance of the subsurface physical and chemical structure in regulating the sensitivity of solute concentrations to discharge variations.

It is important to note that in CAMELS-Chem, there are more sites in the eastern than the western US. Between different sites, measurement duration, frequency, and time periods vary for different solutes. Some biogenic solutes were measured using different approaches in different time periods. These data inconsistencies can influence the values of parameters including A, B, R_0, and C_{eq}. Despite these uncertainties, mean concentrations of all 16 solutes consistently decrease with increasing discharge, underscoring the first-order control of mean discharge. We therefore expect the general conclusion will remain the same when more data become available.

4.2. Distinct Controls of Long-Term C_mQ_m Versus Short-Term CQ Patterns

The long-term, cross-site C_mQ_m patterns here differ from the short-term, within-site instantaneous CQ patterns ($C = aQ^b$) at event to monthly time scales. The latter reflects instantaneous river chemistry to short term hydrological changes whereas the former carries signature of baseline response to climate conditions. The instantaneous CQ patterns have been studied extensively whereas the cross-site C_mQ_m patterns have received scarce attention (Godsey et al., 2019; Maher & Chamberlain, 2014; White & Blum, 1995). The instantaneous concentrations of geogenic solutes have shown dilution patterns with concentrations decreasing with increasing discharge (Ibarra et al., 2016; Torres & Baronas, 2021; Zhi et al., 2020). Instantaneous concentrations of DOC however have seen increase with discharge in more than 80% of the US sites (Zarnetske et al., 2018), the opposite of the C_mQ_m pattern here. The instantaneous CQ patterns at individual sites reflect switching flow paths under different hydrological conditions and depth distribution of source water chemistry [Botter et al., 2020; Dwivedi et al., 2018; Ebeling et al., 2021; Knapp et al., 2020; Zhi & Li, 2020]. In other words, instantaneous CQ patterns arise from mechanisms that differ from long-term C_mQ_m patterns. Even if these patterns at different time scales are "apparently" similar, they should not be interpreted as originated from the same mechanisms.

The C_mQ_m patterns of all solutes exhibit dilution patterns, albeit with differences in the forms for solutes with and without thermodynamic limitation and parameter values. This is remarkable given the diverse origin and reactions across solutes, and the wide range of site idiosyncrasies in lithology, soil type, vegetation cover, among other characteristics. This indicates that climate is the most predominant control on baseline concentrations. In contrast, the short-term CQ relationships are mostly governed by switching flow paths and distinct source water chemistry at different depths, characteristics that are more regulated by subsurface physical and biogeochemical properties, or the subsurface structure of the Critical Zone (Sullivan et al., 2022). For example, the extent of concentration variation with instantaneous discharge, quantified as the power law slope b, has been shown to depend on the magnitude of chemical contrasts in shallow soil water and in deeper groundwater, which is in turn regulated by the abundance of materials such as organic matter and weathering materials at different depths (Zhi & Li, 2020). Solutes that are more abundant in shallow soil water tends to exhibit flushing CQ patterns; solutes that are more abundant in deeper groundwater tends to exhibit dilution CQ patterns (Botter et al., 2020; Seibert et al., 2009; Stewart et al., 2022; Zimmer & McGlynn, 2018). Under conditions where only one major flow path exist, or where the shallow and deep subsurface has similar water chemistry, CQ patterns tend to be chemostatic (Zhi et al., 2019).

4.3. The Future of River Chemistry and Water Quality

How does river chemistry change under a changing climate? Climate disasters, including flooding, droughts, and wildfire, can modify material fluxes and water quality (Robinne et al., 2021; Whitehead et al., 2009). Warmer climates are expected to change river discharge, as well as the timing and magnitude of precipitation events, although the extent and direction will vary by region. River discharge is also expected to decrease due to increasing water demand by a growing population (AghaKouchak et al., 2021). Intermittent streams have already seen longer dry periods, especially in the western US (Zipper et al., 2021). Groundwater aquifers are over extracted and

are subject to surface contaminations (Hartmann et al., 2021; Jasechko & Perrone, 2021; Jasechko et al., 2017; Kumar et al., 2020).

A warmer climate can possibly accelerate soil biogeochemical reactions and chemical weathering, although their response to warming depends on a variety of complex and coupled ecosystem processes that generally remain poorly understood (Greaver et al., 2016; Perdrial et al., 2018; Stegen et al., 2011). For example, vegetation structure will shift in response to shifts in precipitation amount and timing, with ensuing effects on water demand and eventually discharge (Keller, 2019). This in turn will influence river chemistry.

Nonetheless, many places have already seen elevating solute concentrations, although it is often challenging to tease apart the convoluted influence of climate versus human drivers (Guo et al., 2019; Kaushal et al., 2013; Lintern et al., 2018; Noacco et al., 2017). Salinity and electrical conductance, a collective measure of geogenic solutes (cations and anions), have been observed to rise in many places across the United States (Kaushal et al., 2018). Riverine DOC has observed increasing trend since 1980s in Europe and North America (Monteith et al., 2007), often attributed to factors including changing climate, recovery from acid rain, and modified land uses (Adler et al., 2021). In places without acid rain and human activities, DOC exhibits elevated concentrations in warmer and drier years, indicating strong climatic influence (Zhi et al., 2020). Dissolved inorganic carbon (DIC) and alkalinity has also seen continued increase (Drake et al., 2020; Kaushal et al., 2013; Najjar et al., 2020; Raymond & Cole, 2003; Zamanian et al., 2018). Low discharge also entails longer residence time (Benettin et al., 2020) and possibly more extensive transformation of nutrients and carbon into greenhouse gases (Campeau et al., 2019).

Using the space-for-time substitution, we can interpret the data and model here for the future climate. Because all sites are minimally impacted by human perturbations, the results particularly speaks to the effects of a changing climate without the convoluted effects of human perturbations. In places that will become wetter, higher discharge can lower solute concentrations but possibly increased fluxes. This in fact has been predicted for nutrient contamination (Sinha et al., 2017). In places that will become drier, mean concentrations are expected to escalate even without human perturbation. The magnitude of concentration change will vary among solutes and hinges upon the sensitivity of concentrations to discharge variations. For example, some solutes (e.g., TOC, DOC, Cl, SO_4) are highly sensitive ($B \sim -1$) whereas other solutes (e.g., Si) will vary less ($B \sim -0.2$). With B values close to -1, mean concentrations of TOC and DOC can double when mean discharge decreases by half. This is alarming as carbon solutes are highly influential in regulating biological activities and sustaining aquatic life in rivers and streams.

The Clean Water Act, the water quality regulation in the US, establishes total maximum daily loads and MCLs in Drinking Water Standards for many solutes discussed here, including cations, nitrate, and carbon solutes (often categorized as chemical or biological oxygen demand). Increasing solute concentrations can elevate costs and energy use for water treatment, and demand renovated or augmented infrastructure for growing treatment demands (Sanders & Webber, 2012). Water quality risks therefore are an important aspect of climate risks and should be accounted for when we consider future adaptation and mitigation strategies.

Data Availability Statement

All data in this analysis are available at the zenodo website: https://zenodo.org/record/6540786#.Yn0GPOjMI2y, DOI: 10.5281/zenodo.6540786, data citation: LiReactiveWater/EarthsFutureLiEtal2022_CAMELS-Chem_WaterQuality_dataset: Dataset_Lietal2022.

Acknowledgments
This work is supported by the National Science Foundation under Grant Nos. NSF-EAR-1724440 and EAR-2012123 to LL, 1724171 and 2012123 to JP and AH, respectively. We acknowledge two anonymous reviewers whose constructive comments have improved the manuscript.

References

Addor, N., Newman, A. J., Mizukami, N., & Clark, M. P. (2017). The CAMELS data set: Catchment attributes and meteorology for large-sample studies. *Hydrology and Earth System Sciences*, *21*(10), 5293–5313. https://doi.org/10.5194/hess-21-5293-2017

Adler, T., Underwood, K. L., Rizzo, D. M., Harpold, A., Sterle, G., Li, L., et al. (2021). Drivers of dissolved organic carbon mobilization from forested headwater catchments: A multi scaled approach. *Frontiers in Water*, *3*, 578608. https://doi.org/10.3389/frwa.2021.578608

AghaKouchak, A., Mirchi, A., Madani, K., Di Baldassarre, G., Nazemi, A., Alborzi, A., et al. (2021). Anthropogenic drought: Definition, challenges, and opportunities. *Reviews of Geophysics*, *59*(2), e2019RG000683.

Bales, R. C., Molotch, N. P., Painter, T. H., Dettinger, M. D., Rice, R., & Dozier, J. (2006). Mountain hydrology of the Western United States. *Water Resources Research*, *42*(8). https://doi.org/10.1029/2005wr004387

Benettin, P., Fovet, O., & Li, L. (2020). Nitrate removal and young stream water fractions at the catchment scale. *Hydrological Processes*, *34*(12), 2725–2738. https://doi.org/10.1002/hyp.13781

Berner, E. K., & Berner, R. A. (2012). *Global environment. Water, air and geochemical cycles*. Princeton and Oxford: Princeton University Press.
Bernhardt, E. S., Heffernan, J. B., Grimm, N. B., Stanley, E. H., Harvey, J. W., Arroita, M., et al. (2018). The metabolic regimes of flowing waters. *Limnology & Oceanography*, *63*(S1), S99–S118. https://doi.org/10.1002/lno.10726
Bluth, G. J. S., & Kump, L. R. (1994). Lithologic and climatologic controls of river chemistry. *Geochimica et Cosmochimica Acta*, *58*(10), 2341–2359. https://doi.org/10.1016/0016-7037(94)90015-9
Botter, M., Li, L., Hartmann, J., Burlando, P., & Fatichi, S. (2020). Depth of solute generation is a dominant control on concentration-discharge relations. *Water Resources Research*, *56*(8), e2019WR026695. https://doi.org/10.1029/2019wr026695
Boyer, E. W., Hornberger, G. M., Bencala, K. E., & McKnight, D. M. (1997). Response characteristics of DOC flushing in an alpine catchment. *Hydrological Processes*, *11*(12), 1635–1647. https://doi.org/10.1002/(sici)1099-1085(19971015)11:12<1635::aid-hyp494>3.0.co;2-h
Brantley, S. L., Lebedeva, M. I., Balashov, V. N., Singha, K., Sullivan, P. L., & Stinchcomb, G. (2017). Toward a conceptual model relating chemical reaction fronts to water flow paths in hills. *Geomorphology*, *277*, 100–117. https://doi.org/10.1016/j.geomorph.2016.09.027
Brookfield, A. E., Hansen, A. T., Sullivan, P. L., Czuba, J. A., Kirk, M. F., Li, L., et al. (2021). Predicting algal blooms: Are we overlooking groundwater? *The Science of the Total Environment*, *769*, 144442. https://doi.org/10.1016/j.scitotenv.2020.144442
Budyko, M. I. (1974). *Climate and life*. New York, NY: Academic Press.
Campeau, A., Bishop, K., Amvrosiadi, N., Billett, M. F., Garnett, M. H., Laudon, H., et al. (2019). Current forest carbon fixation fuels stream CO_2 emissions. *Nature Communications*, *10*(1), 1876. https://doi.org/10.1038/s41467-019-09922-3
Castellano, M. J., Schmidt, J. P., Kaye, J. P., Walker, C., Graham, C. B., Lin, H., & Dell, C. J. (2010). Hydrological and biogeochemical controls on the timing and magnitude of nitrous oxide flux across an agricultural landscape. *Global Change Biology*, *16*(10), 2711–2720.
Chen, X., & Sivapalan, M. (2020). Hydrological basis of the Budyko curve: Data-guided exploration of the mediating role of soil moisture. *Water Resources Research*, *56*(10), e2020WR028221. https://doi.org/10.1029/2020wr028221
Cleveland, C. C., & Liptzin, D. (2007). C:N:P stoichiometry in soil: Is there a "Redfield ratio" for the microbial biomass? *Biogeochemistry*, *85*(3), 235–252. https://doi.org/10.1007/s10533-007-9132-0
Crawford, J. T., Hinckley, E.-L. S., Litaor, M. I., Brahney, J., & Neff, J. C. (2019). Evidence for accelerated weathering and sulfate export in high alpine environments. *Environmental Research Letters*, *14*(12), 124092. https://doi.org/10.1088/1748-9326/ab5d9c
Davidson, E. A., Belk, E., & Boone, R. D. (1998). Soil water content and temperature as independent or confounded factors controlling soil respiration in a temperate mixed hardwood forest. *Global Change Biology*, *4*(2), 217–227. https://doi.org/10.1046/j.1365-2486.1998.00128.x
Dingman, S. L. (2015). *Physical hydrology* (3rd ed.), (p.657). Long Grove, IL: Waveland Press, Inc.
Dodds, W. K. (2006). Eutrophication and trophic state in rivers and streams. *Limnology & Oceanography*, *51*(1), 671–680. https://doi.org/10.4319/lo.2006.51.1_part_2.0671
Drake, T. W., Podgorski, D. C., Dinga, B., Chanton, J. P., Six, J., & Spencer, R. G. M. (2020). Land-use controls on carbon biogeochemistry in lowland streams of the Congo Basin. *Global Change Biology*, *26*(3), 1374–1389. https://doi.org/10.1111/gcb.14889
Dupas, R., Jomaa, S., Musolff, A., Borchardt, D., & Rode, M. (2016). Disentangling the influence of hydroclimatic patterns and agricultural management on river nitrate dynamics from sub-hourly to decadal time scales. *The Science of the Total Environment*, *571*, 791–800. https://doi.org/10.1016/j.scitotenv.2016.07.053
Duvert, C., Butman, D. E., Marx, A., Ribolzi, O., & Hutley, L. B. (2018). CO_2 evasion along streams driven by groundwater inputs and geomorphic controls. *Nature Geoscience*, *11*(11), 813–818. https://doi.org/10.1038/s41561-018-0245-y
Dwivedi, D., Steefel, C. I., Arora, B., Newcomer, M., David Moulton, J., Dafflon, B., et al. (2018). Geochemical exports to river from the intrameander hyporheic zone under transient hydrologic conditions: East River mountainous watershed, Colorado. *Water Resources Research*, *54*(10), 8456–8477. https://doi.org/10.1029/2018wr023377
Ebeling, P., Kumar, R., Weber, M., Knoll, L., Fleckenstein, J. H., & Musolff, A. (2021). Archetypes and controls of riverine nutrient export across German catchments. *Water Resources Research*, *57*(4), e2020WR028134. https://doi.org/10.1029/2020wr028134
Gaillardet, J., Dupré, B., Louvat, P., & Allègre, C. J. (1999). Global silicate weathering and CO_2 consumption rates deduced from the chemistry of large rivers. *Chemical Geology*, *159*(1–4), 3–30. https://doi.org/10.1016/s0009-2541(99)00031-5
Gentine, P., D'Odorico, P., Lintner, B. R., Sivandran, G., & Salvucci, G. (2012). Interdependence of climate, soil, and vegetation as constrained by the Budyko curve. *Geophysical Research Letters*, *39*(19). https://doi.org/10.1029/2012gl053492
Godsey, S. E., Hartmann, J., & Kirchner, J. W. (2019). Catchment chemostasis revisited: Water quality responds differently to variations in weather and climate. *Hydrological Processes*, *33*(24), 3056–3069.
Godsey, S. E., Kirchner, J. W., & Clow, D. W. (2009). Concentration–discharge relationships reflect chemostatic characteristics of US catchments. *Hydrological Processes*, *23*(13), 1844–1864. https://doi.org/10.1002/hyp.7315
Greaver, T. L., Clark, C. M., Compton, J. E., Vallano, D., Talhelm, A. F., Weaver, C. P., et al. (2016). Key ecological responses to nitrogen are altered by climate change. *Nature Climate Change*, *6*(9), 836–843. https://doi.org/10.1038/nclimate3088
Guo, D., Lintern, A., Webb, J. A., Ryu, D., Liu, S., Bende-Michl, U., et al. (2019). Key factors affecting temporal variability in stream water quality. *Water Resources Research*, *55*(1), 112–129. https://www.doi.org/10.1029/2018wr023370
Hartmann, A., Jasechko, S., Gleeson, T., Wada, Y., Andreo, B., Barberá, J. A., et al. (2021). Risk of groundwater contamination widely underestimated because of fast flow into aquifers. *Proceedings of the National Academy of Sciences*, *118*(20), e2024492118. https://doi.org/10.1073/pnas.2024492118
Herndon, E. M., Dere, A. L., Sullivan, P. L., Norris, D., Reynolds, B., & Brantley, S. L. (2015). Landscape heterogeneity drives contrasting concentration-discharge relationships in shale headwater catchments. *Hydrology and Earth System Sciences*, *19*(8), 3333–3347. https://doi.org/10.5194/hess-19-3333-2015
Higuera, P. E., & Abatzoglou, J. T. (2021). Record-setting climate enabled the extraordinary 2020 fire season in the Western United States. *Global Change Biology*, *27*(1), 1–2. https://doi.org/10.1111/gcb.15388
Hooper, R. P., Christophersen, N., & Peters, N. E. (1990). Modelling streamwater chemistry as a mixture of soilwater end-members—An application to the Panola Mountain catchment, Georgia, U.S.A. *Journal of Hydrology*, *116*(1–4), 321–343. https://doi.org/10.1016/0022-1694(90)90131-g
Hutchins, R. H. S., Tank, S. E., Olefeldt, D., Quinton, W. L., Spence, C., Dion, N., et al. (2020). Fluvial CO_2 and CH_4 patterns across wildfire-disturbed ecozones of subarctic Canada: Current status and implications for future change. *Global Change Biology*, *26*(4), 2304–2319. https://doi.org/10.1111/gcb.14960
Ibarra, D. E., Caves, J. K., Moon, S., Thomas, D. L., Hartmann, J., Chamberlain, C. P., & Maher, K. (2016). Differential weathering of basaltic and granitic catchments from concentration–discharge relationships. *Geochimica et Cosmochimica Acta*, *190*, 265–293. https://doi.org/10.1016/j.gca.2016.07.006
Ibarra, D. E., Rugenstein, J. K. C., Bachan, A., Baresch, A., Lau, K. V., Thomas, D. L., et al. (2019). Modeling the consequences of land plant evolution on silicate weathering. *American Journal of Science*, *319*(1), 1–43. https://doi.org/10.2475/01.2019.01

IPCC. (2021). *Climate change: The physical science basis. Contribution of Working Group I to the Sixth Assessment. Report of the Intergovernmental Panel on Climate Change*, (Vol. 1, p. 300).
Jasechko, S., & Perrone, D. (2021). Global groundwater wells at risk of running dry. *Science*, *372*(6540), 418–421. https://doi.org/10.1126/science.abc2755
Jasechko, S., Perrone, D., Befus, K. M., Bayani Cardenas, M., Ferguson, G., Gleeson, T., et al. (2017). Global aquifers dominated by fossil groundwaters but wells vulnerable to modern contamination. *Nature Geoscience*, *10*(6), 425–+.
Kaushal, S. S., Likens, G. E., Pace, M. L., Utz, R. M., Haq, S., Gorman, J., & Grese, M. (2018). Freshwater salinization syndrome on a continental scale. *Proceedings of the National Academy of Sciences*, *115*(4), E574–E583.
Kaushal, S. S., Likens, G. E., Utz, R. M., Pace, M. L., Grese, M., & Yepsen, M. (2013). Increased river alkalinization in the eastern U.S. *Environmental Science & Technology*, *47*(18), 10302–10311. https://doi.org/10.1021/es401046s
Keller, C. K. (2019). Carbon exports from terrestrial ecosystems: A critical-zone framework. *Ecosystems*, *22*(8), 1691–1705. https://doi.org/10.1007/s10021-019-00375-9
Kim, J. H., Jobbágy, E. G., Richter, D. D., Trumbore, S. E., & Jackson, R. B. (2020). Agricultural acceleration of soil carbonate weathering. *Global Change Biology*, *26*(10), 5988–6002. https://doi.org/10.1111/gcb.15207
Kirchner, J. W. (2009). Catchments as simple dynamical systems: Catchment characterization, rainfall-runoff modeling, and doing hydrology backward. *Water Resoures Research*, *45*(2). https://doi.org/10.1029/2008wr006912
Knapp, J. L. A., von Freyberg, J., Studer, B., Kiewiet, L., & Kirchner, J. W. (2020). Concentration–discharge relationships vary among hydrological events, reflecting differences in event characteristics. *Hydrology and Earth System Sciences*, *24*(5), 2561–2576. https://doi.org/10.5194/hess-24-2561-2020
Kumar, R., Heße, F., Rao, P. S. C., Musolff, A., Jawitz, J. W., Sarrazin, F., et al. (2020). Strong hydroclimatic controls on vulnerability to subsurface nitrate contamination across Europe. *Nature Communications*, *11*(1), 6302. https://doi.org/10.1038/s41467-020-19955-8
Lasaga, A. C. (1998). *Kinetic theory in the earth sciences*, (p. 811). Princeton: Princeton University Press.
Lasaga, A. C., Soler, J. M., Ganor, J., Burch, T. E., & Nagy, K. L. (1994). Chemical-weathering rate laws and global geochemical cycles. *Geochimica et Cosmochimica Acta*, *58*(10), 2361–2386. https://doi.org/10.1016/0016-7037(94)90016-7
Laudon, H., Buttle, J., Carey, S. K., McDonnell, J., McGuire, K., Seibert, J., et al. (2012). Cross-regional prediction of long-term trajectory of stream water DOC response to climate change. *Geophysical Research Letters*, *39*(18). https://doi.org/10.1029/2012gl053033
Li, L. (2019). Watershed reactive transport. In J. Druhan, & C. Tournassat (Eds.), *Reviews in mineralogy & geochemistry: Reactive transport in natural and engineered systems*. Mineralogical Society of America. https://doi.org/10.2138/rmg.2018.85.13
Li, L., Sullivan, P. L., Benettin, P., Cirpka, O. A., Bishop, K., Brantley, S. L., et al. (2021). Toward catchment hydro-biogeochemical theories, *WIREs Water*, *8*(1), e1495. https://doi.org/10.1002/wat2.1495
Lin, H. S., Kogelmann, W., Walker, C., & Bruns, M. A. (2006). Soil moisture patterns in a forested catchment: A hydropedological perspective. *Geoderma*, *131*(3), 345–368.
Lintern, A., Webb, J. A., Ryu, D., Liu, S., Bende-Michl, U., Waters, D., et al. (2018). Key factors influencing differences in stream water quality across space. *WIREs Water*, *5*(1), e1260. https://doi.org/10.1002/wat2.1260
Lloyd, J., & Taylor, J. A. (1994). On the temperature dependence of soil respiration. *Functional Ecology*, *8*(3), 315–323. https://doi.org/10.2307/2389824
Macpherson, G. L., & Sullivan, P. L. (2019). Dust, impure calcite, and phytoliths: Modeled alternative sources of chemical weathering solutes in shallow groundwater. *Chemical Geology*, *527*, 118871.
Mahecha, M. D., Reichstein, M., Carvalhais, N., Lasslop, G., Lange, H., Seneviratne, S. I., et al. (2010). Global convergence in the temperature sensitivity of respiration at ecosystem level. *Science*, *329*(5993), 838–840. https://doi.org/10.1126/science.1189587
Maher, K. (2011). The role of fluid residence time and topographic scales in determining chemical fluxes from landscapes. *Earth and Planetary Science Letters*, *312*(1–2), 48–58. https://doi.org/10.1016/j.epsl.2011.09.040
Maher, K., & Chamberlain, C. P. (2014). Hydrologic regulation of chemical weathering and the geologic carbon cycle. *Science*, *343*(6178), 1502–1504. https://doi.org/10.1126/science.1250770
Moatar, F., Abbott, B. W., Minaudo, C., Curie, F., & Pinay, G. (2017). Elemental properties, hydrology, and biology interact to shape concentration-discharge curves for carbon, nutrients, sediment, and major ions. *Water Resources Research*, *53*(2), 1270–1287. https://doi.org/10.1002/2016wr019635
Moatar, F., Floury, M., Gold, A. J., Meybeck, M., Renard, B., Ferréol, M., et al. (2020). Stream solutes and particulates export regimes: A new framework to optimize their monitoring. *Frontiers in Ecology and Evolution*, *7*(516). https://doi.org/10.3389/fevo.2019.00516
Monger, H. C., Kraimer, R. A., Khresat, S. e., Cole, D. R., Wang, X., & Wang, J. (2015). Sequestration of inorganic carbon in soil and groundwater. *Geology*, *43*(5), 375–378. https://doi.org/10.1130/g36449.1
Monteith, D. T., Stoddard, J. L., Evans, C. D., de Wit, H. A., Forsius, M., Høgåsen, T., et al. (2007). Dissolved organic carbon trends resulting from changes in atmospheric deposition chemistry. *Nature*, *450*, 537. https://doi.org/10.1038/nature06316
Moosdorf, N., Hartmann, J., & Dürr, H. H. (2010). Lithological composition of the North American continent and implications of lithological map resolution for dissolved silica flux modeling. *Geochemistry, Geophysics, Geosystems*, *11*(11). https://doi.org/10.1029/2010gc003259
Najjar, R. G., Herrmann, M., Cintrón Del Valle, S. M., Friedman, J. R., Friedrichs, M. A. M., Harris, L. A., et al. (2020). Alkalinity in tidal tributaries of the Chesapeake Bay. *Journal of Geophysical Research: Oceans*, *125*(1), e2019JC015597. https://doi.org/10.46427/gold2020.1885
Noacco, V., Wagener, T., Worrall, F., Burt, T. P., & Howden, N. J. K. (2017). Human impact on long-term organic carbon export to rivers. *Journal of Geophysical Research: Biogeosciences*, *122*(4), 947–965. https://doi.org/10.1002/2016jg003614
Paschalis, A., Fatichi, S., Zscheischler, J., Ciais, P., Bahn, M., Boysen, L., et al. (2020). Rainfall manipulation experiments as simulated by terrestrial biosphere models: Where do we stand? *Global Change Biology*, *26*(6), 3336–3355. https://doi.org/10.1111/gcb.15024
Perdrial, J., Brooks, P. D., Swetnam, T., Lohse, K. A., Rasmussen, C., Litvak, M., et al. (2018). A net ecosystem carbon budget for snow dominated forested headwater catchments: Linking water and carbon fluxes to critical zone carbon storage. *Biogeochemistry*, *138*(3), 225–243. https://doi.org/10.1007/s10533-018-0440-3
Perdrial, J. N., Mcintosh, J., Harpold, A., Brooks, P., Zapata-Rios, X., Ray, J., et al. (2014). Stream water carbon controls in seasonally snow-covered mountain catchments: Impact of inter-annual variability of water fluxes, catchment aspect and seasonal processes. *Biogeochemistry*, *118*(1), 273–290. https://doi.org/10.1007/s10533-013-9929-y
Pinder, G. F., & Jones, J. F. (1969). Determination of the ground-water component of peak discharge from the chemistry of total runoff. *Water Resources Research*, *5*(2), 438–445. https://doi.org/10.1029/wr005i002p00438
Raymond, P. A., & Cole, J. J. (2003). Increase in the export of alkalinity from North America's largest river. *Science*, *301*(5629), 88–91. https://doi.org/10.1126/science.1083788

Raymond, P. A., Hartmann, J., Lauerwald, R., Sobek, S., McDonald, C., Hoover, M., et al. (2013). Global carbon dioxide emissions from inland waters. *Nature*, *503*(7476), 355–359. https://doi.org/10.1038/nature12760

Raymond, P. A., Oh, N.-H., Turner, R. E., & Broussard, W. (2008). Anthropogenically enhanced fluxes of water and carbon from the Mississippi River. *Nature*, *451*(7177), 449–452. https://doi.org/10.1038/nature06505

Reaver, N. G. F., Kaplan, D. A., Klammler, H., & Jawitz, J. W. (2020). Reinterpreting the Budyko framework. *Hydrology and Earth System Sciences Discussions*, *2020*, 1–31.

Rinaldo, A., Benettin, P., Harman, C. J., Hrachowitz, M., McGuire, K. J., van der Velde, Y., et al. (2015). Storage selection functions: A coherent framework for quantifying how catchments store and release water and solutes. *Water Resources Research*, *51*(6), 4840–4847. https://doi.org/10.1002/2015wr017273

Robinne, F.-N., Hallema, D. W., Bladon, K. D., Flannigan, M. D., Boisramé, G., Bréthaut, C. M., et al. (2021). Scientists' warning on extreme wildfire risks to water supply. *Hydrological Processes*, *35*(5), e14086. https://doi.org/10.1002/hyp.14086

Salehikhoo, F., Li, L., & Brantley, S. L. (2013). Magnesite dissolution rates at different spatial scales: The role of mineral spatial distribution and flow velocity. *Geochimica et Cosmochimica Acta*, *108*(0), 91–106. https://doi.org/10.1016/j.gca.2013.01.010

Sanders, K. T., & Webber, M. E. (2012). Evaluating the energy consumed for water use in the United States. *Environmental Research Letters*, *7*(3), 034034. https://doi.org/10.1088/1748-9326/7/3/034034

Seibert, J., Grabs, T., Köhler, S., Laudon, H., Winterdahl, M., & Bishop, K. (2009). Linking soil- and stream-water chemistry based on a Riparian Flow-Concentration Integration Model. *Hydrology and Earth System Sciences*, *13*(12), 2287–2297. https://doi.org/10.5194/hess-13-2287-2009

Sinha, E., Michalak, A. M., & Balaji, V. (2017). Eutrophication will increase during the 21st century as a result of precipitation changes. *Science*, *357*(6349), 405–408. https://doi.org/10.1126/science.aan2409

Sprenger, M., Stumpp, C., Weiler, M., Aeschbach, W., Allen, S. T., Benettin, P., et al. (2019). The demographics of water: A review of water ages in the critical zone. *Reviews of Geophysics*, *57*(3), 800–834. https://doi.org/10.1029/2018rg000633

Steefel, C. I. (2007). Geochemical kinetics and transport. In J. K. S. Brantley, & A. White (Eds.), *Kinetics of water-rock interaction* (pp. 545–589). New York: Springer.

Stegen, J. C., Swenson, N. G., Enquist, B. J., White, E. P., Phillips, O. L., Jørgensen, P. M., et al. (2011). Variation in above-ground forest biomass across broad climatic gradients. *Global Ecology and Biogeography*, *20*(5), 744–754. https://doi.org/10.1111/j.1466-8238.2010.00645.x

Sterle, G., Perdrial, J., Li, L., Adler, T., Underwood, K., Rizzo, D., et al. (2022). CAMELS-Chem: Augmenting CAMELS (Catchment Attributes and Meteorology for Large-sample Studies) with atmospheric and stream water chemistry data. *Hydrology and Earth System Sciences Discussions*, *2022*, 1–23.

Stewart, B., Shanley, J. B., Kirchner, J. W., Norris, D., Adler, T., Bristol, C., et al. (2022). Streams as mirrors: Reading subsurface water chemistry from stream chemistry. *Water Resources Research*, *58*(1), e2021WR029931. https://doi.org/10.1029/2021wr029931

Sullivan, P. L., Billings, S. A., Hirmas, D., Li, L., Zhang, X., Ziegler, S., et al. (2022). Embracing the dynamic nature of soil structure: A paradigm illuminating the role of life in critical zones of the Anthropocene. *Earth-Science Reviews*, *225*, 103873. https://doi.org/10.1016/j.earscirev.2021.103873

Tetzlaff, D., Seibert, J., McGuire, K. J., Laudon, H., Burns, D. A., Dunn, S. M., & Soulsby, C. (2009). How does landscape structure influence catchment transit time across different geomorphic provinces? *Hydrological Processes*, *23*(6), 945–953. https://doi.org/10.1002/hyp.7240

Torres, M. A., & Baronas, J. J. (2021). Modulation of riverine concentration-discharge relationships by changes in the shape of the water transit time distribution. *Global Biogeochemical Cycles*, *35*(1), e2020GB006694. https://doi.org/10.1029/2020gb006694

Van Meter, K. J., Van Cappellen, P., & Basu, N. B. (2018). Legacy nitrogen may prevent achievement of water quality goals in the Gulf of Mexico. *Science*, *360*(6387), 427–430. https://doi.org/10.1126/science.aar4462

Wen, H., Brantley, S. L., Davis, K. J., Duncan, J. M., & Li, L. (2021). The limits of homogenization: What hydrological dynamics can a simple model represent at the catchment scale? *Water Resources Research*, *57*(6), e2020WR029528. https://doi.org/10.1029/2020wr029528

Wen, H., & Li, L. (2017). An upscaled rate law for magnesite dissolution in heterogeneous porous media. *Geochimica et Cosmochimica Acta*, *210*, 289–305. https://doi.org/10.1016/j.gca.2017.04.019

Wen, H., & Li, L. (2018). An upscaled rate law for mineral dissolution in heterogeneous media: The role of time and length scales. *Geochimica et Cosmochimica Acta*, *235*, 1–20. https://doi.org/10.1016/j.gca.2018.04.024

Wen, H., Perdrial, J., Abbott, B. W., Bernal, S., Dupas, R., Godsey, S. E., et al. (2020). Temperature controls production but hydrology regulates export of dissolved organic carbon at the catchment scale. *Hydrology and Earth System Sciences*, *24*(2), 945–966. https://doi.org/10.5194/hess-24-945-2020

White, A. F., & Blum, A. E. (1995). Effects of climate on chemical weathering in watersheds. *Geochimica et Cosmochimica Acta*, *59*(9), 1729–1747. https://doi.org/10.1016/0016-7037(95)00078-e

Whitehead, P. G., Wilby, R. L., Battarbee, R. W., Kernan, M., & Wade, A. J. (2009). A review of the potential impacts of climate change on surface water quality. *Hydrological Sciences Journal*, *54*(1), 101–123. https://doi.org/10.1623/hysj.54.1.101

Wittenberg, H. (1999). Baseflow recession and recharge as nonlinear storage processes. *Hydrological Processes*, *13*(5), 715–726. https://doi.org/10.1002/(sici)1099-1085(19990415)13:5<715::aid-hyp775>3.0.co;2-n

Wlostowski, A. N., Molotch, N., Anderson, S. P., Brantley, S. L., Chorover, J., Dralle, D., et al. (2021). Signatures of hydrologic function across the critical zone observatory network. *Water Resources Research*, e2019WR026635.

Worrall, F., & Burt, T. P. (2007). Flux of dissolved organic carbon from U.K. rivers. *Global Biogeochemical Cycles*, *21*(1). https://doi.org/10.1029/2006gb002709

Wymore, A. S., Brereton, R. L., Ibarra, D. E., Maher, K., & McDowell, W. H. (2017). Critical zone structure controls concentration-discharge relationships and solute generation in forested tropical montane watersheds. *Water Resources Research*, *53*(7), 6279–6295. https://doi.org/10.1002/2016wr020016

Xiao, D., Shi, Y., Brantley, S. L., Forsythe, B., DiBiase, R., Davis, K., & Li, L. (2019). Streamflow generation from catchments of contrasting lithologies: The role of soil properties, topography, and catchment size. *Water Resources Research*, *55*(11), 9234–9257. https://doi.org/10.1029/2018WR023736

Yan, Z., Bond-Lamberty, B., Todd-Brown, K. E., Bailey, V. L., Li, S., Liu, C., & Liu, C. (2018). A moisture function of soil heterotrophic respiration that incorporates microscale processes. *Nature Communications*, *9*(1), 2562.

Yao, Y., Tian, H., Shi, H., Pan, S., Xu, R., Pan, N., & Canadell, J. G. (2020). Increased global nitrous oxide emissions from streams and rivers in the Anthropocene. *Nature Climate Change*, *10*(2), 138–142. https://doi.org/10.1038/s41558-019-0665-8

Zamanian, K., Pustovoytov, K., & Kuzyakov, Y. (2016). Pedogenic carbonates: Forms and formation processes. *Earth-Science Reviews*, *157*, 1–17. https://doi.org/10.1016/j.earscirev.2016.03.003

Zamanian, K., Zarebanadkouki, M., & Kuzyakov, Y. (2018). Nitrogen fertilization raises CO_2 efflux from inorganic carbon: A global assessment. *Global Change Biology*, *24*(7), 2810–2817. https://doi.org/10.1111/gcb.14148

Zarnetske, J. P., Bouda, M., Abbott, B. W., Saiers, J., & Raymond, P. A. (2018). Generality of hydrologic transport limitation of watershed organic carbon flux across ecoregions of the United States. *Geophysical Research Letters*, *45*(21), 11702–711711. https://doi.org/10.1029/2018gl080005

Zhi, W., Feng, D., Tsai, W.-P., Sterle, G., Harpold, A., Shen, C., & Li, L. (2021). From hydrometeorology to river water quality: Can a deep learning model predict dissolved oxygen at the continental scale? *Environmental Science & Technology*, *55*(4), 2357–2368. https://doi.org/10.1021/acs.est.0c06783

Zhi, W., & Li, L. (2020). The shallow and deep hypothesis: Subsurface vertical chemical contrasts shape nitrate export patterns from different land uses. *Environmental Science & Technology*, *54*(19), 11915–11928. https://doi.org/10.1021/acs.est.0c01340

Zhi, W., Li, L., Dong, W., Brown, W., Kaye, J., Steefel, C., & Williams, K. H. (2019). Distinct source water chemistry shapes contrasting concentration-discharge patterns. *Water Resources Research*, *55*(5), 4233–4251. https://doi.org/10.1029/2018wr024257

Zhi, W., Williams, K. H., Carroll, R. W. H., Brown, W., Dong, W., Kerins, D., & Li, L. (2020). Significant stream chemistry response to temperature variations in a high-elevation mountain watershed. *Communications Earth & Environment*, *1*(1), 43. https://doi.org/10.1038/s43247-020-00039-w

Zimmer, M. A., & McGlynn, B. L. (2018). Lateral, vertical, and longitudinal source area connectivity drive runoff and carbon export across watershed scales. *Water Resources Research*, *54*(3), 1576–1598. https://doi.org/10.1002/2017wr021718

Zipper, S. C., Hammond, J. C., Shanafield, M., Zimmer, M., Datry, T., Nathan Jones, C., et al. (2021). Pervasive changes in stream intermittency across the United States. *Environmental Research Letters*, *16*(8), 084033. https://doi.org/10.1088/1748-9326/ac14ec